Supercond. Sci. Technol. **20** (2007) 1009–1014 doi:10.1088/0953-2048/20/10/020

Trapped field and temperature rise on a ϕ 65 mm GdBaCuO bulk by pulse field magnetization

Hiroyuki Fujishiro, Tetsuya Tateiwa, Kosuke Kakehata, Takuya Hiyama and Tomoyuki Naito

Faculty of Engineering, Iwate University, 4-3-5 Ueda, Morioka 020-8551, Japan

E-mail: fujishiro@iwate-u.ac.jp

Received 13 June 2007, in final form 31 July 2007
Published 31 August 2007
Online at stacks.iop.org/SUST/20/1009

Abstract

The trapped field B_T and temperature rise ΔT on a large GdBaCuO superconducting bulk (65 mm in diameter) have been investigated during pulse field magnetization (PFM), and compared with those on GdBaCuO bulk with a diameter of 45 mm. The maximum trapped field at the bulk center B_T(C) on the ϕ 65 mm bulk is as small as 1.9 T at $T_s = 40$ K for the single pulse field application of $B_{ex} = 6.7$ T, which is smaller than that of the ϕ 45 mm bulk (B_T(C) = 3.2 T). The total trapped flux Φ_T on the ϕ 65 mm bulk is, however, about twice as large as that on the ϕ 45 mm bulk. The magnetic fluxes cannot sufficiently intrude into the center of the ϕ 65 mm bulk at $T_s = 40$ K for pulse field applications up to 6.7 T, whereas a large number of the magnetic fluxes are trapped at the peripheral region of the bulk. The trapped field characteristics for both bulks with different diameters can be roughly interpreted by a simple critical state model under zero field cooling (ZFC).

1. Introduction

For practical applications of a high-temperature superconducting bulk as a quasi-permanent magnet, pulse field magnetization (PFM) instead of conventional field cooled magnetization (FCM) has been intensively investigated because of the inexpensive and mobile experimental setup involved [1]. The trapped field ${B_T}^P$ found using PFM was considered to be low, compared with the trapped field ${B_T}^{FC}$ from FCM due to the large temperature rise caused by the dynamical motion of the magnetic fluxes. The ${B_T}^P$ value was improved at around 77 K by multi-pulse techniques such as an iterative magnetizing operation with gradually reduced pulse field amplitude (IMRA) [2] and a multi-pulse technique with stepwise cooling (MPSC) [3]. At a bulk temperatures T_s as low as 30–40 K, however, ${B_T}^P$ was still low. We have systematically investigated the time and spatial dependence of trapped field ${B_T}^P(t, x)$ and temperature rise $\Delta T(t, x)$ for various applied pulse fields B_{ex}, temperatures T_s, and the various superconducting bulks with different pinning ability [4–6]. To enhance ${B_T}^P$, it was found that both lowering of T_s and lowering of ΔT must be realized at the same time during the PFM procedure. However, ΔT is generally large at lower T_s due to the large heat generation by the large pinning force F_p and/or the small heat capacity of the bulk. Based on the obtained results, we proposed a new PFM method, called a modified multi-pulse technique combined with stepwise cooling (MMPSC) [7]. Using the MMPSC method, which consists of two-stage PFM procedures, we have succeeded in producing a highest field trapping of ${B_T}^P = 5.20$ T on the GdBaCuO bulk (45 mm in diameter), which is a record high ${B_T}^P$ by PFM to date [8]. This method has been proved to be a universal and effective method to enhance ${B_T}^P$ using other bulks such as the SmBaCuO bulk disk (ϕ 45 mm) [9] and the rectangular-shaped GdBaCuO bulk ($33 \times 33 \times 15$ mm^3) [10].

Recently, a superconducting bulk with diameter larger than 60 mm appeared on the commercial market, and a single-grain bulk with 140 mm diameter can also be realized [11]. The trapped field B_T and the total trapped flux Φ_T increase with increasing diameter of the bulk disk, if the critical current density J_c of the bulk superconductor is identical [12]. Then, a superconducting bulk with large diameter is useful for practical

Table 1. The specification of the used bulks and pulse coils.

Bulk name	ϕ 65 mm bulk	ϕ 45 mm bulk
Bulk species	GdBaCuO	GdBaCuO
Diameter (mm)	65	45
Height (mm)	18	18
$B_T{}^{FC}$ (T) at 77 K	1.90	1.72
Used pulse coil	Coil L	Coil S
I.D. (mm)	99	83
O.D. (mm)	121	114
Height (mm)	61	50
Inductance, L (mH)	1.08	1.07
Resistance, R (Ω)	0.28	0.26
Turns	103	112

applications such as in electric motors and generators. Kimura *et al* reported the trapped field $B_T{}^P = 0.8$ T on the ϕ 60 mm GdBaCuO bulk at 77 K using a vortex-type pulsed coil, which was, however, smaller than that on ϕ 45 mm bulk [13]. The application of the PFM technique to the large bulk at lower T_s is desired. However, there are no systematic data of $B_T{}^P$ by PFM for the large bulks.

In the present paper, we investigate the trapped field characteristics on the ϕ 65 mm GdBaCuO bulk at temperatures lower than 77 K. We compare the results with those for the ϕ 45 mm GdBaCuO bulk, and discuss the applicability of the PFM technique for superconducting bulks with large diameter.

2. Experimental details

Highly c-axis-oriented GdBaCuO bulk disks with ϕ 65 mm and ϕ 45 mm (18 mm in thickness; Nippon Steel) were magnetized by the PFM method. Table 1 shows the specification of the bulks and the used pulse coils. The bulks are composed of $GdBa_2Cu_3O_y$ (Gd123) and Gd_2BaCuO_5 (Gd211) with a molar ratio of Gd123:Gd211 = 1.0:0.4, 10.0 wt% Ag_2O and 0.5 wt% Pt. The trapped field $B_T{}^{FC}$ by the FCM method at the center surface of the ϕ 65 mm bulk was 1.9 T at 77 K. Figure 1(a) shows the experimental setup around the ϕ 65 mm bulk and the pulse coil. The bulk was mounted on a soft iron yoke 40 mm in diameter and 20 mm in thickness and tightly anchored onto the cold stage of a Gifford–McMahon (GM) cycle helium refrigerator (Sumitomo Heavy Industry). The bulk was evacuated in the vacuum chamber and was cooled to the temperature from $T_s = 60$ down to 30 K. The bulk was magnetized using the condenser bank (60 mF) and the solenoid pulse coil, which is abbreviated to Coil L, dipped in liquid N_2. A soft-iron cylinder (65 mm in diameter and 40 mm in thickness) was inserted in the Coil L and was faced to the bulk in the vacuum chamber. The rise time of the pulse field generated by the Coil L was $t_r = 12$ ms and the pulse duration was $t_d = 120$ ms. Two Hall sensors (F W Bell, model BHT 921) were attached at positions C (bulk center) and E (20 mm from the bulk center) on the bulk surface. The time evolutions of the local fields [$B_L(C)(t)$ and $B_L(E)(t)$] were monitored using a digital oscilloscope. The trapped field $B_T(C)$ was defined as $B_L(C)(t \rightarrow \infty)$. The temperatures, $T1$, $T2$, and $T3$ were measured at the positions shown in figure 1(a) on the bulk surface using a fine thermocouple.

Figure 1(b) shows the experimental setup around the ϕ 45 mm bulk and the pulse coil (Coil S). $B_T{}^{FC}$ at the center surface of the ϕ 45 mm bulk was 1.72 T at 77 K. The bulk was cooled to $T_s = 40$ K using the same refrigerator and was magnetized using Coil S. The rise time of the pulse field generated by the Coil S was $t_r = 11$ ms and the pulse duration was $t_d = 80$ ms, both of which are somewhat shorter than those of Coil L due to the small inductance and resistance of the coil. Two Hall sensors were attached at positions C (bulk center) and E (15 mm from the bulk center) on the bulk surface. The time evolutions of the local fields [$B_L(C)(t)$ and $B_L(E)(t)$] were monitored. The time dependences of temperatures $T1$–$T3$ on the bulk surface were measured.

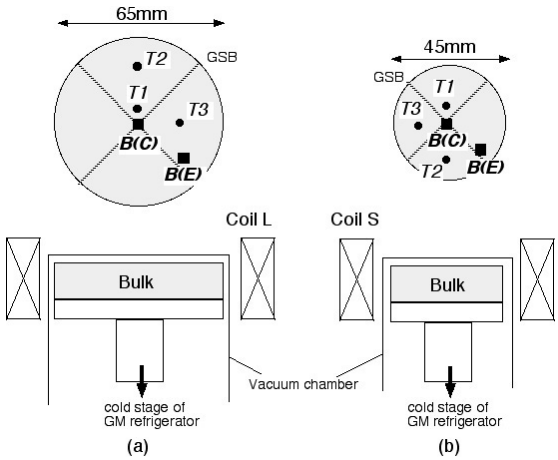

Figure 1. The experimental setup of the (a) ϕ 65 mm GdBaCuO bulk and pulse coil (Coil L), and (b) ϕ 45 mm GdBaCuO bulk and pulse coil (Coil S). The dimension of the bulks and coils are shown in table 1. The measuring positions of magnetic fields (B(C) and B(E)) and temperatures ($T1$, $T2$, and $T3$) after applying the magnetic pulse are indicated.

For both bulks, the applied field $\mu_0 H_a(t)$, of which the maximum strength was defined as B_{ex}, was monitored by observing the current $I(t)$ flowing through the shunt resistor. The B_{ex} value was changed up to 6.7 T, which was a maximum B_{ex} in the present experimental apparatus. The total trapped magnetic flux $\Phi_T(5$ mm) parallel to the c-axis of the bulk was measured using an axial-type Hall sensor, which scanned stepwise on the vacuum chamber 5 mm above the bulk surface with a pitch of 1.2 mm.

3. Results and discussion

3.1. Single pulse application

Figure 2 shows the trapped field $B_T(C)$ at the bulk center of the ϕ 65 mm bulk as a function of the applied field B_{ex} at $T_s = 60$, 40 and 30 K. The results of the ϕ 45 mm bulk at $T_s = 40$ K are also shown. For the ϕ 65 mm bulk, $B_T(C)$ at $T_s = 60$ K starts to increase at around $B_{ex} = 3.2$ T, and increases with increasing B_{ex}. $B_T(C)$ takes a maximum of 1.9 T at $B_{ex} = 6$ T and then decreases for higher B_{ex}. For the pulse field application of the identical strength of B_{ex}, $B_T(C)$ decreases with lowering T_s due to the increase of the pinning force F_p. At $T_s = 40$ and 30 K, magnetic fluxes start to intrude into the bulk center for B_{ex} higher than 4 T and 5 T, respectively. On the other hand, for the ϕ 45 mm bulk at

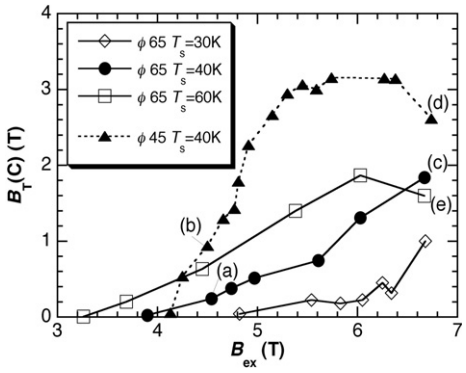

Figure 2. The trapped field B_T(C) at the center of the ϕ 65 mm GdBaCuO bulk as a function of the applied pulse field B_{ex} at $T_s = 60$, 40 and 30 K. For comparison, the results of the ϕ 45 mm GdBaCuO bulk at $T_s = 40$ K are also shown. The marks from (a) to (e) point to the conditions at which the time dependences of the applied field $\mu_0 H_a(t)$ and the local fields B_L(C)(t), B_L(E)(t) are indicated in figure 3 (see text).

$T_s = 40$ K, the magnetic fluxes start to reach the bulk center for $B_{ex} \geqslant 4.2$ T, which is slightly higher than that for the ϕ 65 mm bulk. B_T(C) for the ϕ 45 mm bulk steeply increases with increasing B_{ex}, takes a broad maximum of B_T(C) = 3.2 T at $B_{ex} = 6$ T and then decreases. As shown in table 1, $B_T{}^{FC}$ by FCM on the ϕ 65 mm and ϕ 45 mm bulk is 1.9 and 1.72 T at 77 K, respectively, which suggests that the effective J_c of the ϕ 65 mm bulk is lower than that of the ϕ 45 mm bulk because $B_T{}^{FC}$ is nearly proportional to the diameter of the bulk under an identical J_c of the bulk material. Since a diameter of 65 mm is roughly 1.5 times (exactly 1.44 times) larger than a diameter of 45 mm, $B_T{}^{FC}$ on the ϕ 65 mm should be 2.48 T at 77 K, if the bulks are homogeneous and the J_c value of the ϕ 65 mm bulk is equal to that of the ϕ 45 mm bulk. The result, B_T(C), of the ϕ 45 mm bulk is higher than that of the ϕ 65 mm bulk, suggesting that the magnetic fluxes are easy to intrude and be trapped at the center of the bulk with small diameter, even though the effective J_c value, that is, the pinning force F_p is large at an identical T_s.

Figures 3(a)–(e) show the time evolutions of applied field $\mu_0 H_a(t)$ and local fields, B_L(C)(t) and B_L(E)(t) at positions C and E for conditions (a)–(e) shown in figure 2, respectively. In figures 3(a) and (b), the results after applying a pulse field of $B_{ex} = 4.7$ T at $T_s = 40$ K are compared for the ϕ 65 mm and ϕ 45 mm bulks. At the position E in the peripheral region for both bulks, B_L(E)(t) shows a peak with nearly the same height as $\mu_0 H_a(t)$ without any time delay, and then moderately decreases. The magnetic field of B_T(E) = 1.5–2.0 T was finally trapped. However, at the bulk center of the ϕ 65 mm bulk, the magnetic fluxes cannot intrude and are hardly trapped (B_T(C) $\simeq$ 0). For the ϕ 45 mm bulk, a small number of magnetic fluxes intrude into the bulk center; the maximum B_L(C)(t) was only 1.5 T and the final trapped field, B_T(C) was 1.1 T.

In figures 3(c) and (d), the results at $T_s = 40$ K are compared for both bulks after applying a pulse field of $B_{ex} = 6.7$ T, which is the maximum strength of the magnetic pulse in this study. In the periphery region, nearly the same strength of magnetic field as applied field is detected for both bulks. At the bulk center, B_L(C)(t) for the ϕ 65 mm bulk shows a tiny peak of 2.2 T and then finally reaches a trapped field of B_T(C) = 1.8 T. On the other hand, for the ϕ 45 mm bulk, the maximum magnetic field of B_L(C)(t) = 5.7 T, which is slightly smaller than the applied field $\mu_0 H_a(t)$, enters the bulk center and then decreases. The flux jump takes place due to the large temperature rise by the excess applied field, and the final trapped field B_T(C) decreases to 2.4 T.

Figure 3(e) presents similar results for the ϕ 65 mm bulk at $T_s = 60$ K after applying a pulse field of $B_{ex} = 6.7$ T. It should be noted that nearly the same magnetic field B_L(C)(t) as applied field $\mu_0 H_a(t)$ enters the bulk center, which results from the decrease of the pinning force F_p due to the higher T_s. As a result, the magnetic field of B_T(C) = 1.7 T was trapped. The local fields, B_L(C)(t) and B_L(E)(t) on the ϕ 65 mm bulk quickly decrease after rising to a peak, compared with those for the ϕ 45 mm bulk shown in figures 3(b) and (d). This result suggests that the magnetic flux easily escapes due to the local temperature rise for the ϕ 65 mm bulk.

3.2. Temperature rise

To investigate the difference between the trapped field characteristics of ϕ 65 mm and ϕ 45 mm bulks, the temperature changes during the PFM procedure are compared. Figures 4(a) and (b) show the temperature change $T(t)$ after applying a pulse field of $B_{ex} = 4.74$ T at $T_s = 40$ K for the ϕ 65 mm and ϕ 45 mm bulks, respectively. The temperature rise at the periphery region is fast and large. On the other hand, the temperature rise at the bulk center is moderate and relatively small for each bulk, because the magnetic fluxes always intrude into the bulk from the bulk periphery. For the ϕ 65 mm bulk shown in figure 4(a), $T(t)$ changes depending on the measuring positions in the periphery. The temperature rise of $T3$ is larger, which suggests that the magnetic fluxes preferentially move around this position. On the other hand, for the ϕ 45 mm bulk shown in figure 4(b), the temperature changes in $T2$ and $T3$, both of which are situated in the bulk periphery, are moreorless identical and the magnetic fluxes seem to enter uniformly from the bulk periphery. The temperature rise at the bulk center ($T1$) for the ϕ 45 mm bulk is larger than that for the ϕ 65 mm bulk. The generated heat Q is the sum of the pinning loss Q_p due to the flux trap and the viscous loss Q_v due to the flux movement [14]. For the ϕ 45 mm bulk, B_T(C) is larger and the magnetic fluxes move around the center of the bulk with finite velocity. As a result, Q_p is dominant at the center of the bulk. For the ϕ 65 mm bulk, ΔT_{max} at the bulk center ($T1$) is always smaller than that at $T3$, since the magnetic fluxes cannot all reach the bulk center and a large number of magnetic fluxes are trapped at the bulk periphery. For both bulks, the maximum temperature rise ΔT_{max} increases with increasing B_{ex} due to the increase in the flux velocity and decreasing T_s due to the increase in F_p.

3.3. Total trapped flux Φ_T

Figure 5 shows the total trapped flux Φ_T(5 mm) for the ϕ 65 mm and ϕ 45 mm bulks at $T_s = 40$ K as a function of applied field B_{ex}. Φ_T(5 mm) is estimated by the integration of B_T(5 mm) on the vacuum sheath, at which the distance from the bulk surface is 5 mm. Φ_T(5 mm) of the ϕ 65 mm bulk

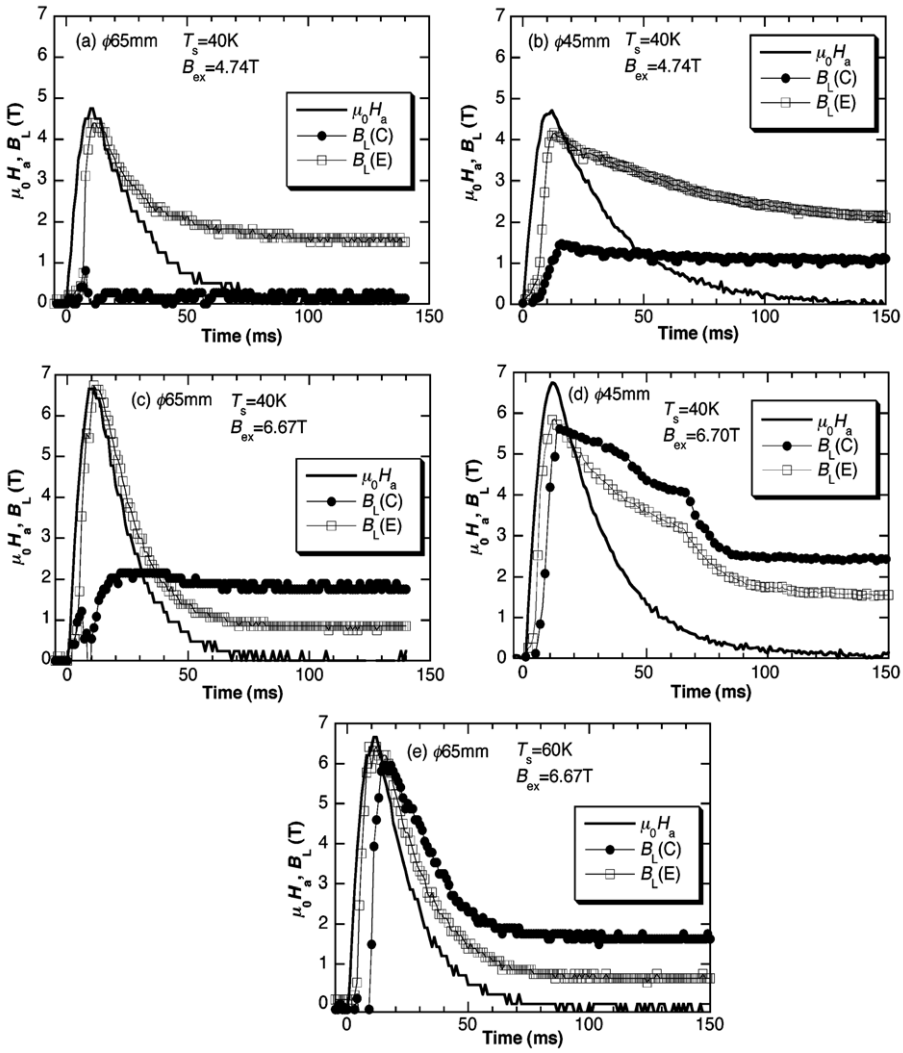

Figure 3. The time dependence of applied field $\mu_0 H_a(t)$ and the local fields $B_L(C)(t)$, $B_L(E)(t)$ at positions C and E of ϕ 65 mm and ϕ 45 mm GdBaCuO bulks for the various conditions of T_s and B_{ex}. Figures (a)–(e) show the results under conditions (a)–(e), which were marked in figure 2.

increases with increasing B_{ex}, takes a maximum at $B_{ex} = 5$ T and then decreases for higher B_{ex}. The $\Phi_T(5\text{ mm})$–B_{ex} curve is different from the $B_T(C)$–B_{ex} curve shown in figure 2; $B_T(C)$ does not take a maximum up to $B_{ex} = 6.7$ T at $T_s = 40$ K. $\Phi_T(5$ mm) of the ϕ 65 mm bulk is about twice as large as that of the ϕ 45 mm bulk, in spite of $B_T(C)$ of the ϕ 65 mm bulk being lower than that of the ϕ 45 mm bulk. These results suggest that the volume of the ϕ 65 mm bulk is about twice as large as that of the ϕ 45 mm bulk and that a large number of the magnetic fluxes are trapped at the bulk periphery. The enhancement of the total trapped flux is a merit for the practical applications of large bulks.

3.4. Sequential pulse application (SPA)

Figure 6 shows the estimated cross section of the trapped field profile on the ϕ 65 mm bulk at $T_s = 40$ K for applying three pulse fields (No. 1–No. 3) with identical strength B_{ex} from 4.74 to 6.74 T, which are applied after recovering to $T_s = 40$ K. In this figure, the trapped field profile was supposed to be symmetrical along the circumferential direction and was roughly estimated using only the measured $B_T(C)$ and $B_T(E)$, and $B_T = 0$ at the bulk edge. For the No. 1 pulse application, the trapped field profile is the concave ('*M-shaped*') profile for $B_{ex} \leqslant 5.61$ T and changes to the convex profile ('cone-shaped') for $B_{ex} \geqslant 6.03$ T. For $B_{ex} = 4.74$ T, $B_T(E)$ increases with increasing number of magnetic pulses, though $B_T(C)$ nearly remains constant. On the other hand, for $B_{ex} = 6.67$ T, $B_T(E)$ decreases with increasing number of magnetic pulses, but $B_T(C)$ slightly increases. The total trapped flux $\Phi_T(5$ mm) after the No. 3 pulse application is shown in figure 5 for the ϕ 65 mm bulk at $T_s = 40$ K as a function of B_{ex}. $\Phi_T(5$ mm) gradually increases with increasing pulse number and is about 30% enhanced after the No. 3 pulse application. For the ϕ 45 mm bulk, both the trapped fields $B_T(C)$ and $B_T(E)$ increase with increasing pulse number and then saturate to final values due to the decrease of ΔT [14]. A similar effect of the Φ_T enhancement was confirmed to be small, possibly due to the small volume of the bulk.

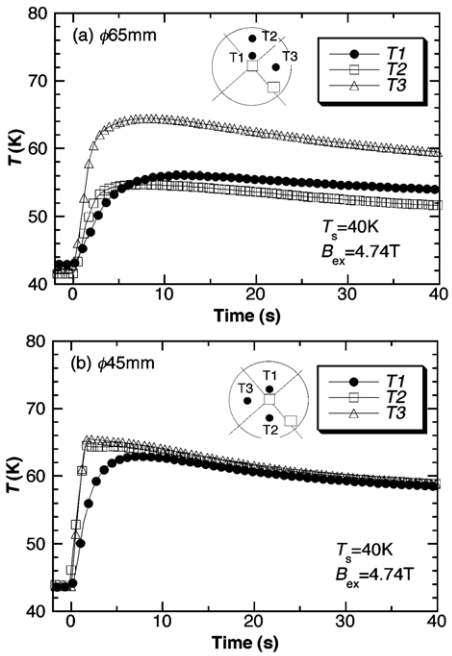

Figure 4. The time dependences of the temperature changes $T(t)$ in $T1$, $T2$, and $T3$ for the (a) ϕ 65 mm and (b) ϕ 45 mm GdBaCuO bulks after applying a pulse field of $B_{ex} = 4.74$ T at $T_s = 40$ K.

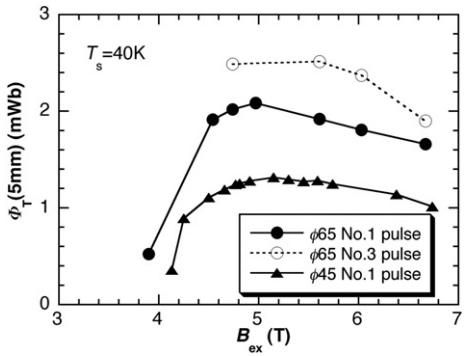

Figure 5. The total trapped flux Φ_T(5 mm) on the ϕ 65 mm and ϕ 45 mm bulks at $T_s = 40$ K as a function of the applied pulse field B_{ex}, which is estimated by the integration of B_T(5 mm), 5 mm above the bulk surface on the vacuum sheath. The Φ_T(5 mm)–B_{ex} curve on the ϕ 65 mm bulk after the No. 3 pulse application with identical strength is also shown (see section 3.4).

3.5. Discussion

A PFM technique can be regarded as a kind of ZFC magnetization; in PFM, the applied magnetic fluxes promptly intrude to the superconducting bulk under the ZFC condition and then some of the magnetic fluxes are trapped and others extrude from the bulk. However, there are some differences; the ZFC magnetization is performed under the quasi-static mode, in which the temperature rise and the flux velocity should be negligible. On the other hand, PFM is performed under the dynamical mode, in which a large heat generation takes place. The flux velocity cannot be negligible and seriously influences the viscous loss Q_v. We discuss the

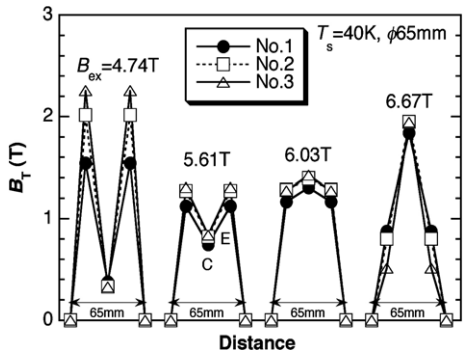

Figure 6. The estimated cross section of the trapped field profile on the ϕ 65 mm bulk at $T_s = 40$ K after applying three successive pulse fields (No. 1–No. 3) with identical strength B_{ex} from 4.74 to 6.67 T.

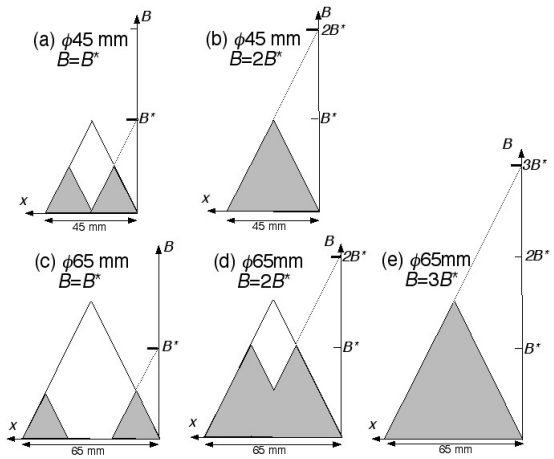

Figure 7. The conceptional view of the trapped field profiles for the ϕ 45 mm bulk ((a) and (b)) and the ϕ 65 mm bulk ((c)–(e)) after the ZFC magnetizing process at constant T_s.

difference in the B_T(C) and the trapped field distribution shown in the previous subsections between ϕ 65 mm and ϕ 45 mm bulks, based on Bean's critical state model [15] as a first approximation. The influence of the temperature rise during the PFM method is also commented.

Figure 7 shows a conceptional view of the trapped field profiles for the ϕ 45 mm (figures (a) and (b)) and ϕ 65 mm bulk (figures (c)–(e)) after the ZFC magnetizing process at constant T_s (for example, $T_s = 40$ K). As shown in section 3.1, the effective J_c value of the ϕ 65 mm bulk was estimated to be lower than that of the ϕ 45 mm bulk. But, for simplicity, we boldly suppose that the J_c value is identical for both bulks, namely, the slope (dB/dx), which is proportional to J_c, is identical [15]. In figure 7, B^* denotes the applied field, at which the ϕ 45 mm bulk is fully magnetized by FCM. In the ZFC magnetization, $2B^*$ must be applied to fully magnetize the ϕ 45 mm bulk. In the ϕ 65 mm bulk, $1.5B^*$ and $3B^*$ are necessary to magnetize fully by the FCM and ZFC magnetizing processes, respectively.

When a magnetic field of B^* is applied to the ϕ 45 mm bulk, the magnetic fluxes just reach the center of the bulk as shown in figure 7(a). On the other hand, the magnetic fluxes

do not reach the center of the ϕ 65 mm bulk as shown in figure 7(c). Figures 7(b) and (d) show the trapped field profiles after applying a magnetic field of $2B^*$. For the ϕ 45 mm bulk shown in figure 7(b), the magnetic fluxes fully enter the bulk center and are trapped with a cone-shaped profile which nearly corresponds to the experimental result for $B_{ex} = 6$ T at $T_s = 40$ K shown in figure 2. On the other hand, for the ϕ 65 mm bulk shown in figure 7(d), the trapped field profile is an '*M-shaped*' one and the B_T(C) at the bulk center is half of that for the ϕ 45 mm bulk. The differences in B_T(C) and the trapped field profile for both bulks with different diameters can be interpreted by the ZFC magnetizing mechanism.

In the practical PFM procedure, however, the explanation mentioned above must be modified slightly, because a large temperature rise takes place. The B^* value and the slope (dB/dx) decrease with increasing temperature. As a result, the height of the cone-shaped profile should be lower. Ito *et al* investigated the trapped field characteristics by PFM, compared with those by ZFC magnetization [16]. They concluded that the dynamical motion of the magnetic fluxes during PFM could be explained by taking into account the significant contribution of the viscous force under heat generation. The slope dB/dx became steeper as it approached the bulk edge due to the viscous force in their experimental results. The average temperature rise in the ϕ 45 mm bulk is nearly equal to that in the ϕ 65 mm bulk, notwithstanding the inhomogeneity in the temperature rise as shown in figure 4. Though the time evolution of the flux distribution during PFM is different from that of the quasi-static ZFC, the final trapped flux distribution by PFM can be qualitatively understood using the behaviors of the ZFC magnetization as shown in figure 7.

If a magnetic pulse field with a magnitude of $3B^*$ is applied to the ϕ 65 mm bulk under ZFC magnetization, B_T(C) is enhanced and the trapped field profile changes from the '*M-shaped*' profile to the 'cone-shaped' one, as shown in figure 7(e). In this case, B_T(C) is 1.5 times larger than that of the ϕ 45 mm bulk ($B_T(C) = 1.5B^*$ for the ϕ 65 mm bulk). Since the power supply, which can generate higher pulse fields, for example $B_{ex} \geqslant 7$ T, is expensive in cost, large in size, and heavy in weight, the use of a large power supply is unrealistic for practical applications. To enhance B_T(C) for the bulk disk with large diameter, an improved PFM technique such as the MMPSC method [16] may be one possible solution.

4. Summary

The trapped field B_T and temperature rise ΔT on large GdBaCuO superconducting bulk (65 mm in diameter) have been investigated during the pulse field magnetization (PFM) method, and compared with those on GdBaCuO bulk with a diameter of 45 mm. The important experimental results and conclusions obtained in this study are summarized as follows.

(1) The maximum trapped field at the bulk center B_T(C) on the ϕ 65 mm bulk is as small as 1.9 T at $T_s = 40$ K for the single pulse field application of $B_{ex} = 6.67$ T, which is smaller than that of the ϕ 45 mm bulk ($B_T(C) = 3.2$ T).
(2) The total trapped flux Φ_T of the ϕ 65 mm bulk is, however, about twice as large as that of the ϕ 45 mm bulk. The magnetic fluxes cannot intrude into the center of the ϕ 65 mm bulk at $T_s = 40$ K sufficiently for the applied pulse field up to 6.7 T, and a large number of the magnetic fluxes are trapped at the peripheral region of the bulk.
(3) The trapped field characteristics for the two bulks with different diameters can be roughly interpreted by a simple critical state model under zero field cooling magnetization.

Acknowledgments

The authors thank Professor Tetsuo Oka of Niigata University, Japan for valuable discussions. This work is supported in part by a Grant-in-Aid for Scientific Research from the Ministry of Education, Culture, Sports, Science, and Technology, Japan (No. 17560001) and from Iwate Prefecture, Japan.

References

[1] Mizutani U, Oka T, Itoh Y, Yanagi Y, Yoshikawa M and Ikuta H 1998 *Appl. Supercond.* **6** 235
[2] Yanagi Y, Itoh Y, Yoshikawa M, Oka T, Hosokawa T, Ishihara H, Ikuta H and Mizutani U 2000 *Advances in Superconductivity XII* (Tokyo: Springer) p 470
[3] Sander M, Sutter U, Koch R and Klaser M 2000 *Supercond. Sci. Technol.* **13** 841
[4] Fujishiro H, Oka T, Yokoyama K and Noto K 2003 *Supercond. Sci. Technol.* **16** 809
[5] Fujishiro H, Yokoyama K, Oka T and Noto K 2004 *Supercond. Sci. Technol.* **17** 51
[6] Fujishiro H, Oka T, Yokoyama K, Kaneyama M and Noto K 2004 *IEEE Trans. Appl. Supercond.* **14** 1054
[7] Fujishiro H, Kaneyama M, Tateiwa T and Oka T 2005 *Japan. J. Appl. Phys.* **44** L1221
[8] Fujishiro H, Tateiwa T, Fujiwara A, Oka T and Hayashi H 2006 *Physica* C **445–448** 334
[9] Fujishiro H, Tateiwa T and Hoyama T 2007 *Japan. J. Appl. Phys.* **46** 4108
[10] Tateiwa T, Sazuka Y, Fujishiro H, Hayashi H, Nagafuchi T and Oka T 2007 *Physica* C at press
[11] Sakai N, Inoue K, Nariki S, Hu A, Murakami M and Hirabayashi I 2005 *Physica* C **426–431** 515
[12] Sakai N, Kita M, Nariki S, Muralidhar M, Inoue K, Hirabayashi I and Murakami M 2006 *Physica* C **445–448** 339
[13] Kimura Y, Matsuzaki H, Ohtani I, Morita E, Izumi M, Sakai N, Hirabayashi I, Miki M, Kitano M and Ida T 2006 *Supercond. Sci. Technol.* **19** S466
[14] Fujishiro H, Yokoyama K, Kaneyama M, Oka T and Noto K 2004 *Physica* C **412–414** 646
[15] Bean C P 1962 *J. Phys. Rev. Lett.* **8** 250
[16] Ito Y and Mizutani U 1996 *Japan. J. Appl. Phys.* **35** 2114